Comprehensive Dynamic Model for the Calculation of the Molecular Weight and Long Chain Branching Distributions in Metallocene-Catalyzed Ethylene Polymerization Reactors

H. Yiannoulakis, A. Yiagopoulos, P. Pladis, and C. Kiparissides*,†

Department of Chemical Engineering and Chemical Process Engineering Research Institute, Aristotle University of Thessaloniki, P.O. Box 472, Thessaloniki, Greece 540 06

Received September 20, 1999; Revised Manuscript Received January 14, 2000

ABSTRACT: In the present study, a dynamic model is developed for the calculation of the molecular weight and long chain branching distributions in a continuous solution metallocene-catalyzed ethylene polymerization reactor. The model is based on the fractionation of the total polymer chain population into a number of classes, each one representing polymer chains having the same long chain branching content. According to the proposed method, dynamic balance equations are derived for the leading moments of each class of polymer chains as well as for the moments of the overall "live", saturated and unsaturated "dead" polymer chain distributions. A two-parameter Schultz−Flory distribution is used to reconstruct the molecular weight distribution (MWD) of individual classes of polymer chains in terms of their leading moments. The overall MWD is calculated by the weighted sum of all class molecular weight distributions. Simulation results are presented to demonstrate the predictive capabilities of the present model and a parametric study is carried out to analyze the effect of the rate constant for long chain branching formation, k_{pLCB}, on the MWD and the average molecular properties of the polymer. The effects of chain transfer agent concentration and reactor mean residence time on the molecular weight and long chain branching distributions of polyethylene are also studied.

Introduction

Metallocene catalysts have revolutionized polyolefin manufacturing since the discovery of methylaluminoxanes as active cocatalysts in the late 1970s. Since then, research efforts have been focused on the production of novel polyolefins with superior and better controllable properties (e.g., impact strength, temperature resistance, hardness, etc.). The main advantage of metallocenes over conventional Ziegler−Natta catalysts is that the former have a single polymerization site which leads to the production of highly stereospecific polyolefins having narrow molecular weight and comonomer distributions. A number of excellent reviews have appeared in the open literature dealing with the various types of metallocene systems, their polymerization mechanisms, and associated molecular properties.[1−5]

Adversely, the benefits arising from the narrow molecular weight distribution of metallocene polymers are counterpoised by inferior polymer processabillity properties. Thus, to enhance polymer melt processability, long chain branches should be incorporated in the polyolefin chains. This can be achieved with the use of constrained geometry metallocene catalysts. The unique feature of these catalysts is the sterically unencumbered nature of the active sites that facilitates the incorporation of bulky macromolecules to the growing polymer chains.[6,7] Lai et al.[8] reported that the constrained geometry catalyst used in the INSITE Technology process, led to the production of polyethylene and ethylene/α-olefin copolymers with varying degrees of long chain branching (e.g., 0.01−3 LCB per 10^3 carbon atoms), while maintaining the polydispersity index below 3.5 and in most cases close to its theoretical minimum value of 2. Swogger[9] reported values of 0.07, 1.28, and 3 LCBs per 10^4 carbon atoms and respective values of 0.2, 0.53, 0.44, and 0.66 LCBs per molecule based on ^{13}C NMR measurements of polyethylenes produced in a solution continuous stirred tank reactor (CSTR) in the presence of a constrained geometry catalyst.

Branched polyolefins can be produced using constrained geometry catalysts in either slurry, gas phase, or solution polymerization reactors. In particular, continuous solution processes utilize soluble constrained geometry catalysts at elevated temperatures and short residence times.[4,8] These reactors usually operate above the melting point of the polymer (e.g., 114−200 °C). As the reactor temperature increases, the rate of incorporation of macromonomers into the linear polymer chains increases too, due to the enhanced mobility of the polymer chains and the increase of the macromonomer formation rate. Moreover, at high temperatures, steric limitations related to the addition of the macromonomer to the active catalyst site are significantly reduced. On the other hand, as the reactor temperature increases, the deactivation rate of active sites increases too, affecting both monomer conversion and the degree of long chain branching.

Soares and Hamielec[10] developed a simple steady-state analytical expression for the prediction of the MWD of branched polyethylene produced in a solution polymerization CSTR using a constrained geometry catalyst. In a follow-up publication, they modified their earlier analytical expression to account for copolymerization kinetics using Stockmayer's bivariate distribution and the pseudo-kinetic rate constant method.[11]

Zhu and Li[12] suggested the use of a binary catalyst system for the production of highly branched polyolefins with a very narrow MWD. They postulated that this binary catalyst system should comprise a single catalyst

* To whom correspondence should be addressed.
† Telephone: + 3031 99 6211.Fax: +31 99 6198. E-mail: cypress@alexandros.cperi.forth.gr.

10.1021/ma9915935 CCC: $19.00
Published on Web 03/10/2000

Table 1. Simplified Kinetic Mechanism of Ethylene Polymerization in the Presence of a Constrained Geometry Metallocene Catalyst[10,12]

description	reaction
activation (by cocatalyst)	$S_p + \text{cocatalyst} \xrightarrow{k_a} P_{0,0}$
initiation/reinitiation	$P_{0,0} + M \xrightarrow{k_i} P_{1,0}$
propagation	$P_{r,m} + M \xrightarrow{k_p} P_{r+1,m}$
long chain branching	$P_{r,m} + D^{=}_{s,n} \xrightarrow{k_{pLCB}} P_{r+s,m+n+1}$
chain transfer (by hydrogen)	$P_{r,m} + H_2 \xrightarrow{k_{trH}} D_{r,m} + P_{0,0}$
chain transfer (by monomer)	$P_{r,m} + M \xrightarrow{k_{trM}} D^{=}_{r,m} + P_{1,0}$
β-H elimination:	$P_{r,m} \xrightarrow{k_\beta} D^{=}_{r,m} + P_{0,0}$
deactivation (1st order):	$P_{r,m} \xrightarrow{k_d} D_{r,m}$

site producing macromonomers having a very narrow distribution and a constrained geometry catalyst for the production of branched polymer chains. In this manner, comb polymers could be synthesized having a high degree of branching and a polydispersity index close to the theoretical minimum of 2. They developed a simple steady-state model for the prediction of the molecular weight distribution and showed that the maximum attainable polydispersity index had a value of 2.25. However, no experimental evidence was provided supporting their theoretical claims.

The present paper is organized as follows: In the next section, rate functions for the net production of "live" and "dead" polymer chains are derived based on a simple constrained geometry catalyst kinetic scheme accounting for long chain branching. Subsequently, dynamic molar balance equations are written for all active species to follow the molecular weight developments in an isothermal continuous solution polymerization reactor. Following the developments of Pladis and Kiparissides,[13] a comprehensive dynamic model based on the numerical fractionation method is proposed for the calculation of the molecular weight and long chain branching distributions. Simulation results are then presented to demonstrate the predictive capabilities of the present model, and a parametric study is carried out to investigate the effect of the rate constant for long chain branching formation, k_{pLCB}, on the MWD and the average properties of the polymer. Finally, the effects of chain transfer agent concentration and reactor mean residence time on the molecular weight and long chain branching distributions of polyethylene are analyzed.

Reaction Kinetics and Design Equations

In a continuous solution polymerization reactor operating at relatively medium pressures (e.g., 30 bar) and elevated temperatures (e.g., 114−200 °C), ethylene can undergo ionic polymerization in the presence of a constrained geometry catalyst/cocatalyst system (e.g., a monocyclopentadienyl transition metal complex and tris(pentafluorophenyl)borane) leading to the formation of branched polymer chains. A simple kinetic mechanism describing the polymerization of ethylene in the presence of a constrained geometry catalyst is depicted in Table 1. The subscripts r and m denote the number of ethylene units and the number of long chain branches in the polymer chain, respectively. The mechanism includes initiation and propagation reactions, a molecular weight control reaction (e.g., transfer to hydrogen), formation of "dead" polymer chains with a terminal double bond via β-hydride elimination and transfer to monomer reactions, formation of trifunctional long chain branches (LCB) via the incorporation of an unsaturated "dead" polymer chain into a growing polymer chain, and a first-order spontaneous deactivation reaction for the active polymer chains. The present kinetic mechanism does not account for a possible higher order deactivation reaction.

Polymerization Rate Functions. Let P_r, D_r, and $D^{=}_r$ be the total concentrations of "live" polymer chains, saturated "dead" polymer chains, and "dead" polymer chains with a terminal double bond, respectively. Let r_{P_r}, r_{D_r} and $r_{D^{=}_r}$ be the corresponding net rates of production of "live" polymer chains, saturated "dead" polymer chains, and unsaturated "dead" polymer chains. On the basis of the postulated kinetic mechanism of ethylene polymerization over a constrained geometry catalyst, one can derive the following expressions for r_{P_r}, r_{D_r} and $r_{D^{=}_r}$ by combining the individual rates of generation and consumption of "live" and "dead" polymer chains.

Net formation rate of "live" polymer chains of length r:

$$r_{P_r} = k_p[M]P_{r-1} + k_{pLCB}\sum_{s=2}^{r-2} D^{=}_s P_{r-s} - (k_p[M] + k_{pLCB}\sum_{s=2}^{\infty} D^{=}_s + k_{trH}[H_2] + k_{trM}[M] + k_\beta + k_d)P_r \quad (1)$$

Net formation rate of saturated "dead" polymer chains of length r:

$$r_{D_r} = (k_{trH}[H_2] + k_d)P_r \quad (2)$$

Net formation rate of unsaturated "dead" polymer chains of length r:

$$r_{D^{=}_r} = (k_\beta + k_{trM}[M])P_r - k_{pLCB}D^{=}_r\sum_{s=1}^{\infty} P_s \quad (3)$$

On the basis of the above rate function definitions, one can easily derive an infinite system of differential equations to describe the molecular weight developments in a polymerization reactor. For modeling purposes, it is often impractical to solve this large system of differential equations describing the conservation of all individual species in the reactor. Thus, a lower order system of differential equations is usually obtained by using the method of moments. This method is based on the statistical representation of the molecular properties of the polymer (e.g., M_n, M_w) in terms of the leading moments of the number chain length distributions of the "live", saturated and unsaturated "dead" polymer chains, defined by the following equations:

$$\lambda_\nu = \sum_{r=1}^{\infty} r^\nu P_r \quad (4)$$

$$\mu_\nu = \sum_{r=2}^{\infty} r^\nu D_r \quad (5)$$

$$\bar{\mu}_\nu = \sum_{r=2}^{\infty} r^\nu \bar{D}_r \tag{6}$$

Accordingly, one can obtain the corresponding rate functions for the moments of the number chain length distributions of the "live", saturated and unsaturated "dead" polymer chains by multiplying each term of eqs 1−3 by the term r^ν and summing up the resulting expressions over the total variation of r. The final moment rate functions are written as follows.

Moment rates of "live" polymer chains:

$$r_{\lambda_0} = k_i P_{0,0}[M] - (k_{trH}[H_2] + k_\beta + k_d)\lambda_0 \tag{7}$$

$$r_{\lambda_1} = (k_p[M] + k_{pLCB}\bar{\mu}_1 + k_{trM}[M])\lambda_0 + k_i P_{0,0}[M] - (k_{trH}[H_2] + k_{trM}[M] + k_\beta + k_d)\lambda_1 \tag{8}$$

$$r_{\lambda_2} = k_p[M](2\lambda_1 + \lambda_0) + k_{pLCB}(2\lambda_1\bar{\mu}_1 + \lambda_0\bar{\mu}_2) + k_i P_{0,0}[M] + k_{trM}[M]\lambda_0 - (k_{trH}[H_2] + k_{trM}[M] + k_\beta + k_d)\lambda_2 \tag{9}$$

Moment rates of saturated "dead" polymer chains:

$$r_{\mu_\nu} = (k_{trH}[H_2] + k_d)\lambda_\nu, \quad \nu = 0, 1, 2 \tag{10}$$

Moment rates of unsaturated "dead" polymer chains:

$$r_{\bar{\mu}_\nu} = (k_\beta + k_{trM}[M])\lambda_\nu - k_{pLCB}\bar{\mu}_\nu\lambda_0, \quad \nu = 0, 1, 2 \tag{11}$$

The other reaction rates of interest (e.g., vacant active sites net formation rate, monomer, and chain transfer agent consumption rates, etc.) will be given by the following expressions.

Net formation rate of vacant active sites:

$$r_{P_{0,0}} = (k_{trH}[H_2] + k_\beta)\lambda_0 - (k_i[M] + k_d)P_{0,0} \tag{12}$$

Monomer consumption rate:

$$r_M = -[M](k_i P_{0,0} + k_p\lambda_0 + k_{trM}\lambda_0) \tag{13}$$

Chain transfer agent consumption rate:

$$r_{H_2} = -[H_2]k_{trH}\lambda_0 \tag{14}$$

LCB formation rate:

$$r_{LCB} = k_{pLCB}\lambda_0\bar{\mu}_0 \tag{15}$$

The various symbols used in the above kinetic expressions are explained in the Notation section.

Reactor Design Equations. A schematic representation of a typical continuous stirred tank solution polymerization reactor for the ethylene polymerization is shown in Figure 1. As can be seen, ethylene, hydrogen, and diluent (e.g., Isopar, a mixture of C_8−C_{10} saturated hydrocarbons) are continuously fed into the reactor. The catalytic metal complex and the cocatalyst are also continuously injected into the reactor via a separate stream. Sufficient mixing time (e.g., 10 s) is allowed for the catalyst and the cocatalyst to react to the desired extent (e.g., catalyst partial or full activation), prior to their injection into the reactor.[8] The reactor exit stream comprises the polyethylene solution and the unreacted ethylene and hydrogen.

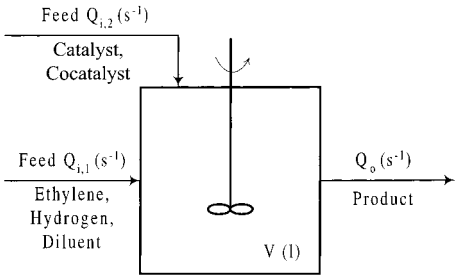

Figure 1. Schematic representation of an ethylene solution polymerization CSTR.

Assuming that the total reaction volume remains constant (e.g., V = constant) and the reaction mixture consists of a single well-mixed phase, the dynamic molar balances for ethylene and hydrogen in the reactor are written as follows:

$$d[M]/dt = (Q_{i,1}[M]_i - Q_o[M])/V + r_M \tag{16}$$

$$d[H_2]/dt = (Q_{i,1}[H_2]_i - Q_o[H_2])/V + r_{H_2} \tag{17}$$

Here, V, [M], and [H_2] denote the volume of the reaction mixture, the monomer concentration and the hydrogen concentration, respectively. $Q_{i,1}$, $Q_{i,2}$, Q_o, r_M and r_{H_2} denote the ethylene−hydrogen−diluent volumetric feed rate, the catalyst−cocatalyst volumetric feed rate and the total outlet volumetric rate from the reactor, and the consumption rates of ethylene and hydrogen given by eqs 13 and 14, respectively.

Since there is sufficient precontacting time between the catalyst and the cocatalyst,[8] it is assumed that the catalyst is fully activated upon injection into the reactor. Thus, the dynamic molar balance for the vacant active sites will be given by

$$dP_{0,0}/dt = (Q_{i,2}P^i_{0,0} - Q_o P_{0,0})/V + r_{P_{0,0}} \tag{18}$$

where $P_{0,0}$ denotes the concentration of vacant active sites in the reactor and $P^i_{0,0}$ is the concentration of vacant active sites in the catalyst−cocatalyst feed stream. $r_{P_{0,0}}$ is the net formation rate of vacant active sites given by eq 12.

Finally, the dynamic molar balances for all other species X (e.g., λ_ν, μ_ν, $\bar{\mu}_\nu$, LCB) in the reactor can be expressed as

$$d[X]/dt = -Q_o[X]/V + r_X \tag{19}$$

where [X] denotes the concentration of species "X" in the reactor, and r_X the net rate of formation of "X" calculated by eqs 7−11 and 15.

The reactor design eqs 16−19 coupled with the appropriate equations (see eqs 7−15), describing the various molar species rates, were numerically solved, using Gear's method, to simulate the dynamic behavior of a continuous solution ethylene polymerization reactor.

Calculation of MWD of Branched Polyethylene

Following the developments of Pladis and Kiparissides,[13] the total polymer chain population is divided into a series of classes, each one representing a subset of polymer chains with the same LCB content (e.g., linear chains, chains with one LCB, chains with two LCB, etc.). According to the proposed method, dynamic balance equations are derived for the leading moments

of each class of polymer chains as well as for the moments of the overall "live", saturated and unsaturated "dead" polymer chain distributions. A two-parameter Schultz−Flory distribution is used to reconstruct the MWD of each class of polymer chains in terms of its leading moments. Finally, the overall MWD is calculated by the weighted sum of all class molecular weight distributions.

Table 1 depicts all the elementary reactions considered in the present kinetic model. The reactions can be divided into two groups. The first group includes reactions which do not change the class number of the reacting macromolecules. The second group of reactions (e.g., reaction with a terminal double bond) leads to the formation of higher classes (e.g., higher LCB content). Notice that the only reaction that increases the class number is that involving the formation of a trifunctional long chain branching point. Following the kinetic scheme described in Table 1, one can calculate the corresponding net formation rates for "live" and "dead" polymer chains for each distinct polymer class.

Net formation rate of linear "live" polymer chains of length r:

$$r_{P_{r,0}} = k_p[M]P_{r-1,0} - (k_p[M] + k_{pLCB}\sum_{s=1}^{\infty}\sum_{n=0}^{\infty}\overline{\overline{D}}_{s,n} + k_{trH}[H_2] + k_{trM}[M] + k_\beta + k_d)P_{r,0} \quad (20)$$

Net formation rate of the "m" class of branched "live" polymer chains of length r:

$$r_{P_{r,m}} = k_p[M]P_{r-1,m} + k_{pLCB}\sum_{i=0}^{m-1}\sum_{s=2}^{r-2}P_{s,i}\overline{\overline{D}}_{r-s,m-1-i} - (k_p[M] + k_{pLCB}\sum_{s=1}^{\infty}\sum_{n=0}^{\infty}\overline{\overline{D}}_{s,n} + k_{trH}[H_2] + k_{trM}[M] + k_\beta + k_d)P_{r,m}, \quad m = 0, 1, 2, ..., N_c \quad (21)$$

Net formation rate of the "m" class of branched saturated "dead" polymer chains of length r:

$$r_{D_{r,m}} = (k_{trH}[H_2] + k_d)P_{r,m}, \quad m = 0, 1, 2, ..., N_c \quad (22)$$

Net formation rate of the "m" class of branched unsaturated "dead" polymer chains of length r:

$$r_{\overline{\overline{D}}_{r,m}} = (k_\beta + k_{trM}[M])P_{r,m} - k_{pLCB}\overline{\overline{D}}_{r,m}\sum_{s=1}^{\infty}\sum_{n=0}^{\infty}P_{s,n}, \quad m = 0, 1, 2, ..., N_c \quad (23)$$

Accordingly, we define the corresponding "live" and "dead" moments for each class of polymer chains:

$$\lambda_{\nu,m} = \sum_{r=1}^{\infty} r^\nu P_{r,m}, \quad m = 0, 1, 2, ..., N_c \quad (24)$$

$$\mu_{\nu,m} = \sum_{r=2}^{\infty} r^\nu D_{r,m}, \quad m = 0, 1, 2, ..., N_c \quad (25)$$

$$\overline{\overline{\mu}}_{\nu,m} = \sum_{r=2}^{\infty} r^\nu \overline{\overline{D}}_{r,m}, \quad m = 0, 1, 2, ..., N_c \quad (26)$$

Following the moment developments presented in the previous section, the class rate equations for the leading moments of the "live" and "dead" polymer chains are derived.

Moment rates for linear "live" polymer chains:

$$r_{\lambda_{0,0}} = k_i P_{0,0}[M] - (k_{trH}[H_2] + k_\beta + k_d + k_{pLCB}\overline{\overline{\mu}}_0)\lambda_{0,0} \quad (27)$$

$$r_{\lambda_{1,0}} = (k_i P_{0,0} + k_{trM}\lambda_0 + k_p\lambda_{0,0})[M] - (k_{trH}[H_2] + k_{trM}[M] + k_\beta + k_d + k_{pLCB}\overline{\overline{\mu}}_0)\lambda_{1,0} \quad (28)$$

$$r_{\lambda_{2,0}} = (k_i P_{0,0} + k_{trM}\lambda_0)[M] + k_p[M](2\lambda_{1,0} + \lambda_{0,0}) - (k_{trH}[H_2] + k_{trM}[M] + k_\beta + k_d + k_{pLCB}\overline{\overline{\mu}}_0)\lambda_{2,0} \quad (29)$$

Moment rates for the "m" class of branched "live" polymer chains:

$$r_{\lambda_{0,m}} = k_{pLCB}\sum_{i=0}^{m-1}\lambda_{0,i}\overline{\overline{\mu}}_{0,m-1-i} - (k_{trH}[H_2] + k_{trM}[M] + k_\beta + k_d + k_{pLCB}\overline{\overline{\mu}}_0)\lambda_{0,m}, \quad m = 1, 2, ..., N_c \quad (30)$$

$$r_{\lambda_{1,m}} = k_p[M]\lambda_{0,m} + k_{pLCB}\sum_{i=0}^{m-1}(\lambda_{1,i}\overline{\overline{\mu}}_{0,m-1-i} + \lambda_{0,i}\overline{\overline{\mu}}_{1,m-1-i}) \quad (31)$$

$$r_{\lambda_{2,m}} = k_p[M](2\lambda_{1,m} + \lambda_{0,m}) + k_{pLCB}\sum_{i=0}^{m-1}(\lambda_{2,i}\overline{\overline{\mu}}_{0,m-1-i} + 2\lambda_{1,i}\overline{\overline{\mu}}_{1,m-1-i} + \lambda_{0,i}\overline{\overline{\mu}}_{2,m-1-i}) - (k_{trH}[H_2] + k_{trM}[M] + k_\beta + k_d + k_{pLCB}\overline{\overline{\mu}}_0)\lambda_{2,m}, \quad = 1, 2, ..., N_c \quad (32)$$

Moment rates for the "m" class of branched saturated "dead" polymer chains:

$$r_{\mu_{\nu,m}} = (k_{trH}[H_2] + k_d)\lambda_{\nu,m}, \quad \nu = 0, 1, 2 \text{ and } m = 0, 1, 2, ..., N_c \quad (33)$$

Moment rates for the "m" class of branched unsaturated "dead" polymer chains:

$$r_{\overline{\overline{\mu}}_{\nu,m}} = (k_\beta + k_{trM}[M])\lambda_{\nu,m} - k_{pLCB}\lambda_0\overline{\overline{\mu}}_{\nu,m}, \quad \nu = 0, 1, 2 \text{ and } m = 0, 1, 2, ..., N_c \quad (34)$$

The molecular weight averages (M_n, M_w), the polydispersity index, and the number of long chain branches per 10^3 carbon atoms or/and per molecule are accordingly calculated in terms of the moments of the total number chain length distributions (TNCLDs) of "live" and "dead" polymer chains.

Number-average molecular weight:

$$M_n = 28 \times DP_n = 28 \times \frac{\lambda_1 + \overline{\overline{\mu}}_1 + \mu_1}{\lambda_0 + \overline{\overline{\mu}}_0 + \mu_0} \quad (35)$$

Weight-average molecular weight:

$$M_w = 28 \times DP_w = 28 \times \frac{\lambda_2 + \overline{\overline{\mu}}_2 + \mu_2}{\lambda_1 + \overline{\overline{\mu}}_1 + \mu_1} \quad (36)$$

Polydispersity index:

$$PD = \frac{M_w}{M_n} \tag{37}$$

Number of long chain branches per 10^3 carbon atoms:

$$\text{LCB/1000 C atoms} = 500 \times [\text{LCB}]/(\lambda_1 + \bar{\bar{\mu}}_1 + \mu_1) \tag{38}$$

Number of long chain branches per molecule:

$$\text{LCB/mol} = [\text{LCB}]/(\lambda_0 + \bar{\bar{\mu}}_0 + \mu_0) \tag{39}$$

Calculation of the MWD. Using the calculated moments, a two-parameter Schultz−Flory distribution can be employed to reconstruct the weight chain length distribution (WCLD) of a class of polymer chains

$$W_m(r) = \frac{y_m(ry_m)^{z_m} e^{-ry_m}}{e^{\ln[\Gamma(z_m+1)]}}, \quad m = 0, ..., N_c \tag{40}$$

where $W_m(r)$ denotes the mass fraction of the polymer chains of class "m" with a degree of polymerization r. The parameters of the two variable distribution will be given by the following expressions:

$$z_m = \frac{\text{DP}_{n,m}}{\text{DP}_{w,m} - \text{DP}_{n,m}}; \quad y_m = \frac{z_m + 1}{\text{DP}_{w,m}} \tag{41}$$

$\text{DP}_{n,m}$ and $\text{DP}_{w,m}$ are the number and weight-average degree of polymerization for the "m" class of polymer chains, respectively. The use of the Schultz−Flory equation, eq 40, for the reconstruction of the WCLD is theoretically justified since the MWD for a class of polymer chains is narrow (e.g., the polydispersity index is lower than 2).

The overall WCLD will be given by the weighted sum of all polymer class distributions:

$$W_{\text{total}}(r) = \sum_{m=0}^{N_c} W_m(r)(\lambda_{1,m} + \bar{\bar{\mu}}_{1,m} + \mu_{1,m})/(\lambda_1 + \bar{\bar{\mu}}_1 + \mu_1) \tag{42}$$

Finally, the respective LCB distributions per molecule and per 10^3 carbon atoms are calculated using the following expressions.

LCB distribution per molecule:

$$W_{\text{LCB/mol}}(r) = \sum_{m=0}^{N_c} m N_{r,m} / \sum_{m=0}^{N_c} N_{r,m}, \quad r = 1, ..., \infty \tag{43}$$

LCB distribution per 10^3 carbon atoms:

$$W_{\text{LCB/10}^3\text{ C atoms}}(r) = 500 \times W_{\text{LCB/mol}}(r)/r, \quad r = 1, ..., \infty \tag{44}$$

$N_{r,m}$ denotes the concentration of the polymer chains in class "m", having a degree of polymerization r and m long chain branches, given by the following expression:

$$N_{r,m} = W_m(r)/r \tag{45}$$

Simulation Results and Discussion

To demonstrate the predictive capabilities of the present model, the dynamic behavior of an ethylene solution polymerization CSTR was considered. Numerical simulations were carried out in order to investigate the effect of the number of classes, the kinetic rate constant ratio k_{pLCB}/k_p, the chain transfer agent concentration, and the reactor mean residence time on the MWD and LCB content of polyethylene produced. Nominal operating conditions and numerical values of the various kinetic parameters, used in the present study, are reported in Table 2.

Table 2. Nominal Operating Conditions[8] and Numerical Values of the Kinetic Parameters Used for the Simulation of an Ethylene Solution Polymerization CSTR in the Presence of a Constrained Geometry Catalyst

reactor parameters	kinetic parameters
$P^i_{0,0}$ (mol/L) = 0.0005	k_i (L mol^{-1} s^{-1}) = 650
$[M]_i$ (mol/L) = 0.855	k_p (L mol^{-1} s^{-1}) = 1.43 × 10^4
$[H_2]_i$ (mol/L) = 0.05	k_{pLCB} (L mol^{-1} s^{-1}) = 720
τ (min) = 15	k_{trH} (L mol^{-1} s^{-1}) = 1.5
$P^i_{0,0}/[Me]_i = 1$	k_{trM} (L mol^{-1} s^{-1}) = 21.4
	k_β (s^{-1}) = 0.8
	k_d (s^{-1}) = 0.001

Effect of the Number of Classes on the Calculated MWD. A typical question concerning the accuracy of the present method is related to the number of classes required to obtain a reliable representation of the MWD of a branched polymer. It is important to point out that the number of classes required for an accurate representation of the MWD can vary considerably depending on the total LCB content. Thus, it was found that for a polyethylene with a low LCB content (e.g., ∼0.35 LCB per molecule), the number of classes required for a reliable reconstruction of the MWD was relatively low (e.g., ∼10). On the other hand, for a polymer with a high LCB content (e.g., 3.5 LCB per molecule), a large number of classes was needed (e.g., ∼85). This means that the computational effort can significantly increase as the LCB content of polyethylene increases.

To ensure that the selected number of classes was sufficient for the accurate reconstruction of the MWD, the following convergence criterion was established:

$$\left|\sum_{m=0}^{N_c}(\mu_{1,m} + \bar{\bar{\mu}}_{1,m}) - (\mu_1 + \bar{\bar{\mu}}_1)\right|/(\mu_1 + \bar{\bar{\mu}}_1) \le \epsilon \tag{46}$$

ϵ is a convergence parameter with typical values in the range $0 < \epsilon \le 0.05$. The present method was assumed to converge to the correct MWD if the total monomer conversion, calculated by the summation of the $\mu_{1,m}$ and $\bar{\bar{\mu}}_{1,m}$ "class" moments, with respect to the total number of "classes", N_c, was approximately equal to the monomer conversion given by the sum of the first moments of the TNCLDs, μ_1 and $\bar{\bar{\mu}}_1$, of the saturated and unsaturated "dead" polymer chains. It was shown that satisfaction of the above convergence criterion (see eq 46) resulted in the correct selection of the number of classes, N_c, needed for the accurate reconstruction of the overall MWD.

In Figure 2 the MWDs of branched polyethylene calculated by the Soares−Hamielec[10] analytical solution and the present method are shown. It can be seen that the two methods produced identical results. However, it is important to point out that the Soares−Hamielec approach refers to the steady-state MWD of the final product while the present method can predict the MWD of the polymer during the transient operation of the reactor. Furthermore, the Soares−Hamielec approach

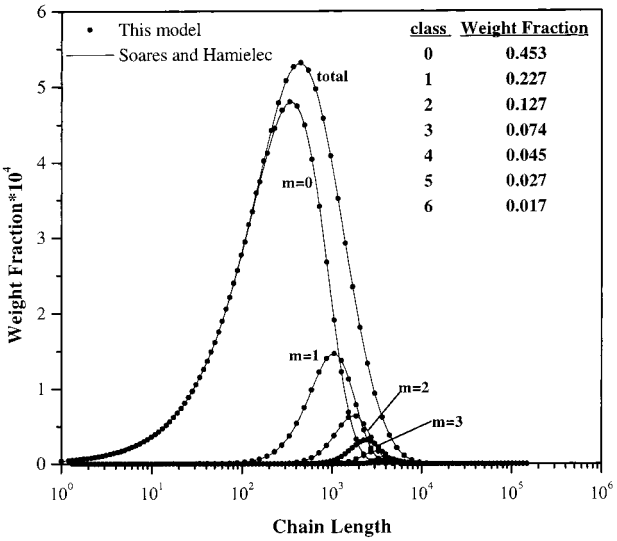

Figure 2. Calculated MWDs at the exit of an ethylene solution polymerization CSTR ($k_\beta = 3.2$ s^{-1}, $k_{trM} = 0$).

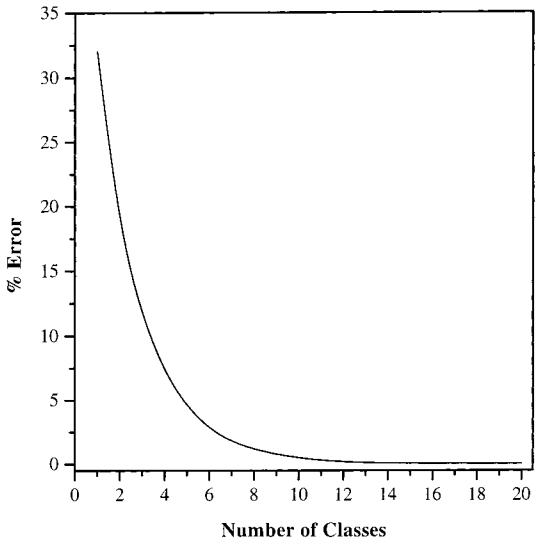

Figure 3. Effect of the number of classes on the convergence error (see eq 46).

does not provide the necessary criteria concerning the number of classes required for the accurate reconstruction of the overall MWD. According to the results of Figure 2, a relatively narrow molecular weight distribution is obtained (e.g., PD = 2.67 and a weight-average molecular weight of ~50 000), corresponding to a polyethylene with a LCB content of ~0.3 LCB per 10^3 carbon atoms. In the same figure, the WCLDs of linear and branched polymer chains are plotted. Notice that the linear polymer chains ($m = 0$) account for about 46% of the total polymer mass, while the corresponding mass fractions of "classes" $m = 1$, 2, and 3 are significantly lower (e.g., 0.23, 0.12, and 0.07, respectively). The remaining classes (e.g., $m > 3$) required for the reconstruction of the total MWD account for less than 12% of the total polymer mass.

Figure 3 illustrates an important computational feature of the present method in direct relation to the results of Figure 2. It depicts the effect of the number of classes on the prediction error, as calculated by eq 46. It is apparent that the prediction error decreases dramatically as the number of classes increases. Notice that the error becomes practically zero when 15 classes

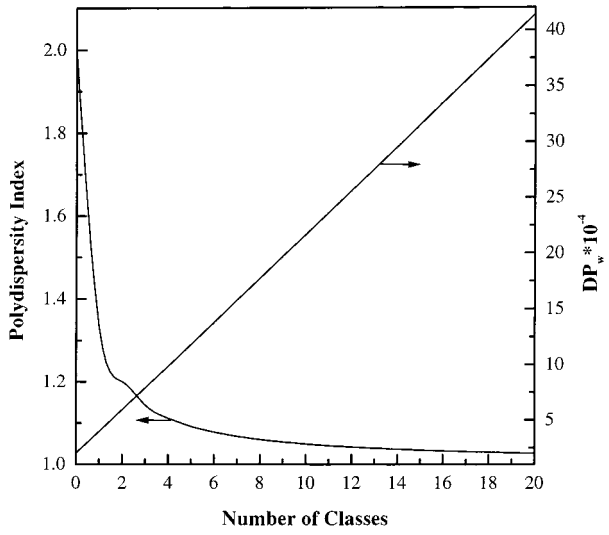

Figure 4. Variation of the polydispersity index and weight-average degree of polymerization of polymer chains in a class with respect to the class number.

are employed for the reconstruction of the total MWD curve.

Figure 4 illustrates the polydispersity index and the weight-average degree of polymerization of each class of polymer chains, in direct relation with the results of Figure 2. It can be seen that the polydispersity index decreases as the class number increases, that is, the LCB content increases. The polydispersity index of highly branched polymer chains asymptotically reaches the value of 1 whereas the polydispersity index of linear polymer chains attains the theoretical value of 2. On the other hand, as the number of long chain branches increases, the weight-average degree of polymerization exhibits a linear increase.

Another important feature of the method presented in this study, is related to the calculation of the LCB distribution of branched polyethylene. Parts a and b of Figure 5 depict the calculated LCB distributions per molecule and per 10^3 carbon atoms, respectively. It can be seen that the number of long chain branches per molecule increases as the degree of polymerization increases (Figure 5a). On the other hand, the number of long chain branches per 10^3 carbon atoms exhibits a maximum at large chain lengths. This is solely due to the different scale used for representing the long chain branching content (e.g., LCB per molecule vs LCB per 10^3 carbon atoms) meaning that when the LCB content is plotted with respect to the number of carbon atoms found in a polymer chain, it does not monotonically increase with respect to the total degree of polymerization.

Figure 6 depicts the time evolution of the overall MWD during the start-up of an ethylene solution polymerization CSTR under the conditions of Table 2. The calculation of the MWD for each class of polymer chains (see eq 40) as well as of the overall WCLD (see eq 42) is carried out at discrete intervals based on the values of the moments for each class of polymer chains. Since the model predicts the dynamic response of all "class" moments, the reconstruction of individual MWDs as well as of the overall WCLD is possible during the dynamic operation of the reactor. It can be seen that the MWD remains unimodal throughout the polymerization. Notice that as the polymerization time increases, the MWD gradually broadens and the high

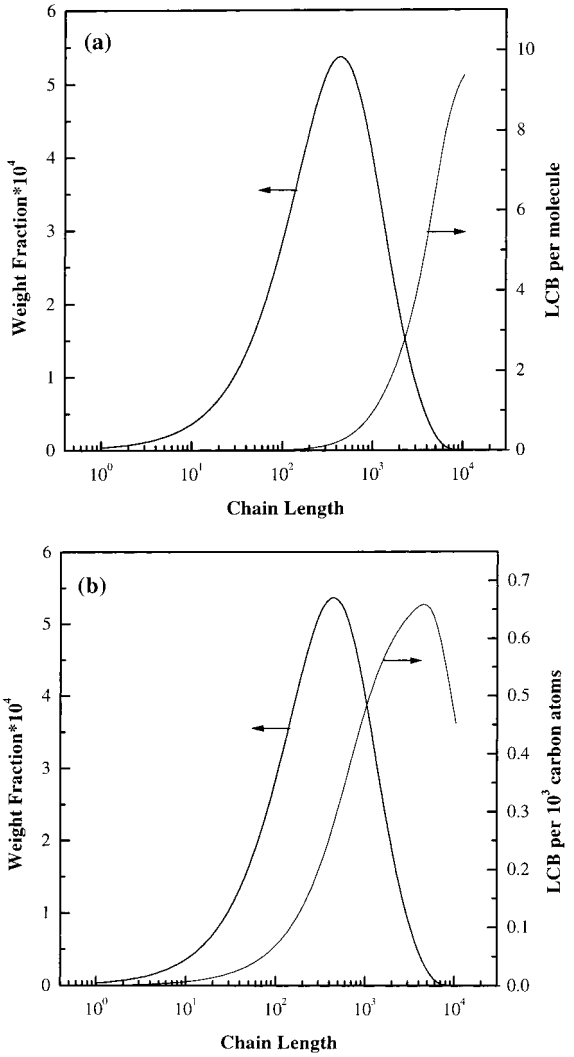

Figure 5. Calculated steady-state distributions of LCB per molecule (a) and LCB per 10^3 carbon atoms (b).

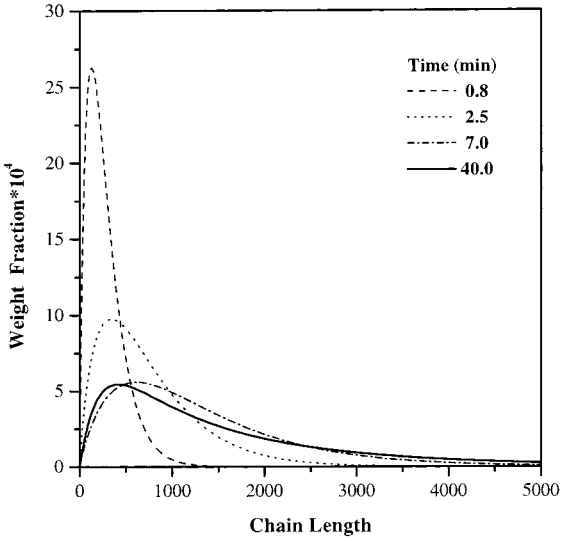

Figure 6. Time variation of the MWD during reactor start-up.

molecular weight tail of the distribution shifts to larger chain lengths. Moreover, parts a and b of Figure 7 show the corresponding time variation of the LCB content and polydispersity index, respectively, during the reactor start-up.

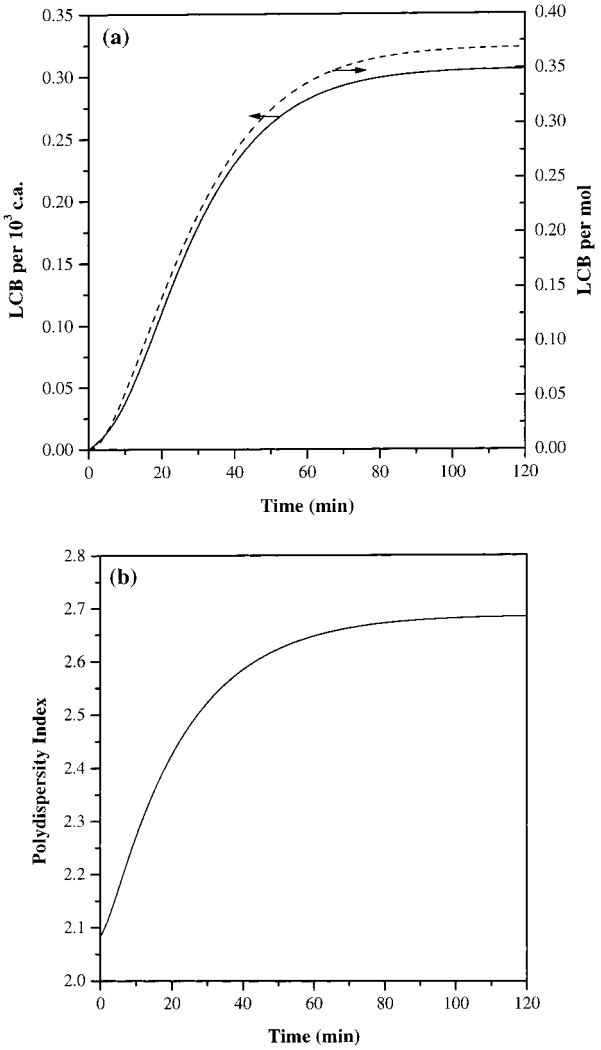

Figure 7. Time variation of the LCB per molecule, LCB per 10^3 carbon atoms (a) and polydispersity index (b) during reactor start-up.

Effect of the k_{pLCB}/k_p Ratio on the MWD. The effect of the ratio of k_{pLCB}/k_p on the LCB content and MWD of the polymer are shown in Figures 8 and 9, respectively. Figure 8 illustrates the effect of the ratio of k_{pLCB}/k_p on the LCB content per 10^3 carbon atoms or/and molecule and the corresponding polydispersity index of the polyethylene. It can be seen that as the ratio k_{pLCB}/k_p increases (e.g., the rate of macromonomer insertion increases), the LCB content and the polydispersity index increase too. Notice that the LCB content per molecule is more sensitive to variations of the k_{pLCB}/k_p ratio than the LCB content per 10^3 carbon atoms. It can be seen that, for a value of the k_{pLCB}/k_p ratio of 0.1, the polydispersity attains a value of 3.5 while the LCB per molecule is equal to 0.75. Finally, Figure 9 depicts the effect of the ratio of k_{pLCB}/k_p on the corresponding MWD of the product. It should be noted that as the ratio of k_{pLCB}/k_p increases the MWD becomes broader.

Effect of the Chain Transfer Agent Concentration on the MWD. The concentration of hydrogen plays an important role in the molecular weight control of the polyolefin. Figure 10 illustrates the effect of the hydrogen feed concentration on the MWD of the polyethylene. It can be seen that as the hydrogen concentration increases (e.g., from 0.05 to 0.3 mol/L), the MWD is shifted to lower chain lengths. The effect of hydrogen

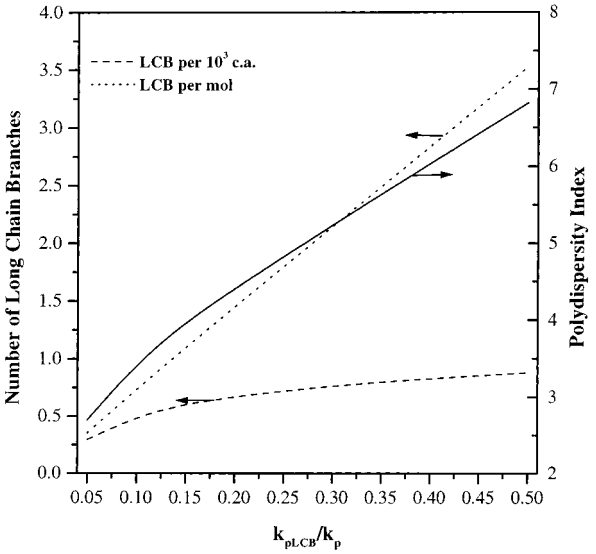

Figure 8. Effect of the k_{pLCB}/k_p ratio on the LCB content of the polymer.

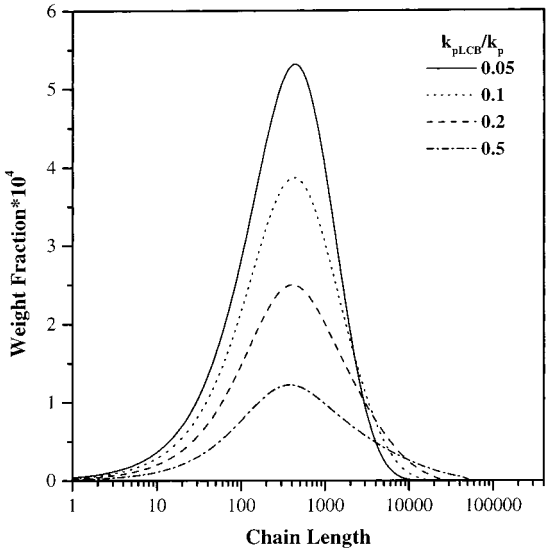

Figure 9. Effect of the k_{pLCB}/k_p ratio on the MWD.

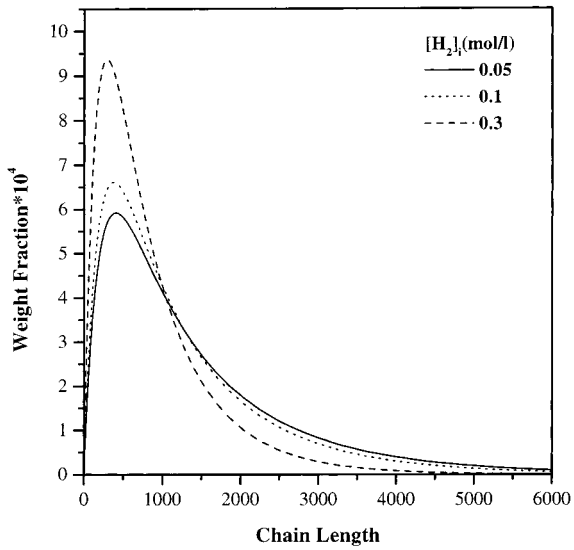

Figure 10. Effect of the feed hydrogen concentration on the MWD.

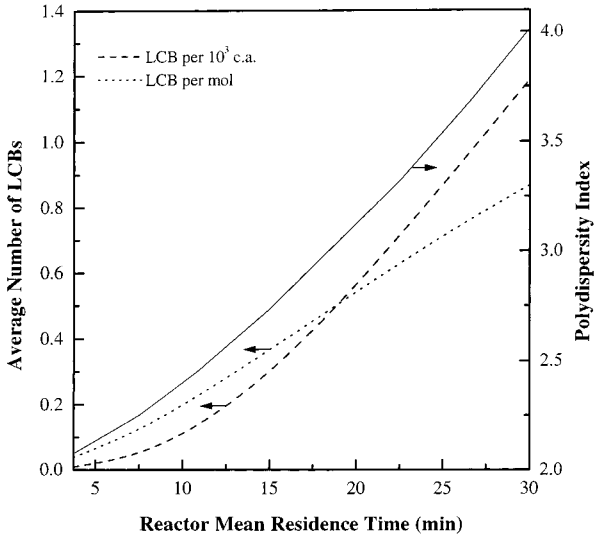

Figure 11. Effect of the reactor mean residence time on the average LCB content of the polymer.

concentration on the average molecular properties of polyethylene is also illustrated in Table 3. Notice that as the hydrogen concentration increases, the LCB content per molecule, the polydispersity index and the number and weight-average molecular weights decrease. On the other hand, the LCB content per 10^3 carbons atoms is practically unaffected (e.g., 0.3) since the hydrogen concentration does not affect the ethylene conversion, thus, the quantity $(\lambda_1 + \bar{\mu}_1 + \mu_1)$ in eq 38 does not change with the hydrogen concentration. Notice that for a hydrogen concentration of 0.3 mol/L, the corresponding polydispersity index takes a value of 2.4. From the results of Table 3, one can conclude the polydispersity index of polyethylene can be lowered while maintaining the same LCB content per 10^3 carbon atoms by increasing the hydrogen concentration in the feed stream.

Table 3. Effect of Hydrogen Feed Concentration on the Average Molecular Properties of Branched Polyethylene

$[H_2]_i$ (mol/L)	LCB/10^3 C atoms	LCB/mol	PD	M_n	M_w
0.05	0.3	0.33	2.67	17 963	47 961
0.1	0.3	0.29	2.59	13 939	36 102
0.3	0.3	0.21	2.40	10 193	24 462

Effect of Reactor Mean Residence Time on the MWD. Another important reactor parameter is the mean residence time of the CSTR. Numerical simulations were carried out in order to investigate the effect of reactor mean residence time on the properties of the polymer product. Figure 11 illustrates the effect of reactor mean residence time on the LCB content and the polydispersity index of polyethylene. As the reactor mean residence time increases the LCB per 10^3 carbon atoms, the LCB per molecule and the polydispersity index increase too, since longer residence times result in an increase of the concentration of unsaturated polymer chains which, in turn, increases the macromonomer insertion rate.

On the other hand, one could expect that the high molecular weight tail of the MWD will be shifted to larger chain lengths as the reactor mean residence time increases due to an increase of the rate of macromonomer insertion.[10] However, as can be seen in Figure 12, an increase of the reactor mean residence time (e.g., from 7.5 to 22.5 min), results in a shift of the MWD to lower chain lengths. This behavior can be explained in

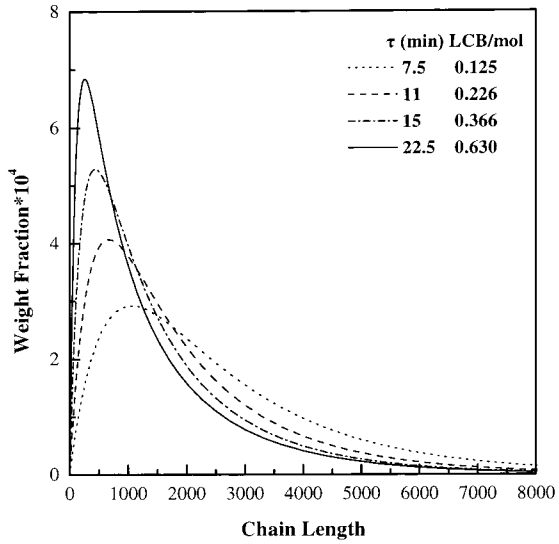

Figure 12. Effect of the reactor mean residence time on the MWD of the polymer.

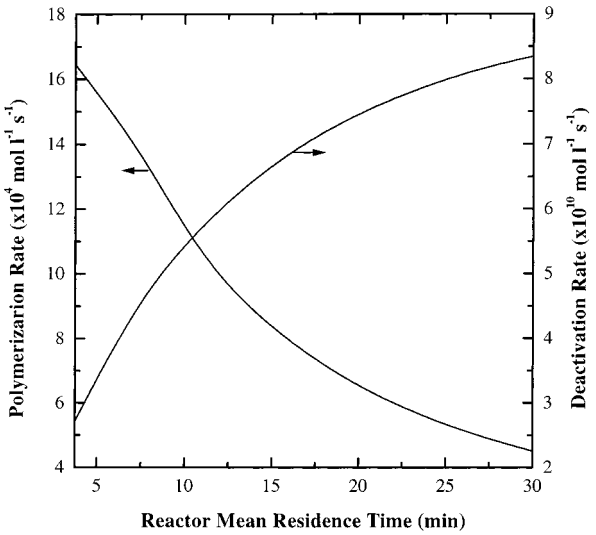

Figure 13. Effect of the reactor mean residence time on the polymerization and deactivation rates.

conjunction with the simulation results of Figures 13 and 14. In Figure 13, the effect of the reactor mean residence time on the polymerization and spontaneous deactivation rates is shown. It can be seen that as the reactor mean residence time increases the polymerization rate decreases rapidly due to the increase of the deactivation rate. Figure 14 illustrates the effect of reactor mean residence time on the corresponding average molecular weights of the polymer in the reactor. It is apparent that an increase of the reactor mean residence time results in a decrease of the molecular weight averages and an increase of the polydispersity index.

Thus, the reactor mean residence time is a key process parameter since it affects the molecular properties of the polyethylene (e.g., M_n, M_w, LCB, PD) as well as the polymerization rate and the monomer conversion in the reactor.

Conclusions

The present work describes the development of a comprehensive dynamic model for the calculation of the molecular weight and long chain branching distributions

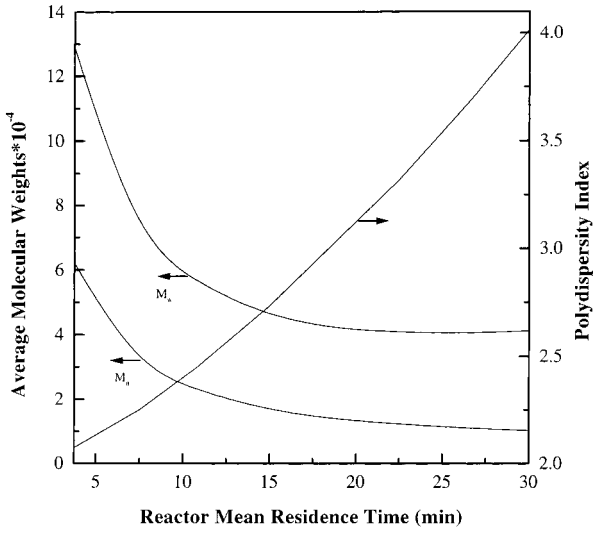

Figure 14. Effect of the reactor mean residence time on the average molecular weights of the polymer.

in metallocene- catalyzed ethylene polymerizations. The numerical fractionation method[13] was employed to reconstruct the overall MWD of the branched polymer.

It was shown that the number of classes used to reconstruct the MWD of branched polyethylene had a significant impact on the accuracy of the present model. It was also shown that polyethylenes with narrow MWDs and relatively high degrees of LCB can be produced in a solution polymerization CSTR using a constrained geometry metallocene catalyst. Moreover, it was found that the polydispersity index of polyethylene could be lowered while the LCB content per 10^3 carbon atoms remained constant, by adjusting the hydrogen concentration in the reactor feed. Finally, it was demonstrated that the reactor mean residence time was a critical process parameter since it affected both the molecular properties of the polymer and the polymerization rate. The results of the present study are of particular importance in the design and optimization of catalytic (e.g., constrained geometry metallocenes) ethylene solution continuous stirred tank polymerization reactors.

Acknowledgment. We gratefully acknowledge the DGXII of the EU for supporting this research under the BRITE/EURAM Project, BE96-3022.

Notation

D_r	concentration of "dead" saturated polymer chains of length r (mol/L)
$D_r^=$	concentration of "dead" polymer chains of length r with a terminal double bond (mol/L)
$D_{r,m}$	concentration of "dead" saturated polymer chains of length r and "m" long chain branches (mol/L)
$D_{r,m}^=$	concentration of "dead" polymer chains of length r, "m" long chain branches, and a terminal double bond (mol/L)
DP_n	number-average degree of polymerization
DP_w	weight-average degree of polymerization
$[H_2]$	hydrogen concentration (mol/L)
k_a	activation rate constant (L mol^{-1} s^{-1})
k_β	β-H elimination rate constant (s^{-1})
k_i	initiation rate constant (L mol^{-1} s^{-1})
k_d	spontaneous deactivation rate constant (s^{-1})

k_p	propagation rate constant (L mol^{-1} s^{-1})
k_{pLCB}	long chain branching rate constant (L mol^{-1} s^{-1})
k_{trH}	chain transfer rate constant (L mol^{-1} s^{-1})
k_{trM}	transfer to monomer rate constant (L mol^{-1} s^{-1})
[M]	monomer concentration (mol/L)
[M_e]	metal concentration (mol/L)
M_n	number-average molecular weight
M_w	weight-average molecular weight
N_c	number of classes
$N_{r,m}$	concentration of polymer chains of length r and m long chain branches (mol/L)
$P_{0,0}$	concentration of vacant active sites (mol/L)
P_r	concentration of "live" polymer chains of length r (mol/L)
$P_{r,m}$	concentration of "live" polymer chains of length r and "m" long chain branches (mol/L)
PD	polydispersity index
Q	volumetric rate (L/s)
S_p	potential active site
r_X	net rate of formation of species "X" (mol L^{-1} s^{-1})
V	reactor volume (L)
[X]	concentration of species "X" (mol/L)
W	weight fraction
λ	"live" polymer moment (mol/L)
μ	"dead" polymer moment (mol/L)
ν	moment order
ρ	density (g/L)

Subscripts and Superscripts

i	feed stream
o	outlet stream
r	chain length
m	class number

Abbreviations

CSTR	continuous stirred tank reactor
LCB	long chain branching
MWD	molecular weight distribution
TNCLD	total number chain length distribution
WCLD	weight chain length distribution

References and Notes

(1) Gupta, V. K.; Satish, S.; Bhardwaj, I. S. *J. Macromol. Sci.—Rev. Macromol. Chem. Phys.* **1994**, *C34*, 439.
(2) Huang, J.; Rempel, G. L. *Prog. Polym. Sci.* **1995**, *20*, 459.
(3) Soares, J. B. P.; Hamielec, A. E. *Polym. React. Eng.* **1995**, *3* (*2*), 131.
(4) Hamielec, A. E.; Soares, J. B. P. *Prog. Polym. Sci.* **1996**, *21*, 651.
(5) Kaminsky, W. *Macromol. Chem. Phys.* **1996**, *197*, 3907.
(6) Woo, T. K.; Fan, L.; Ziegler, T. *Organometallics* **1994**, *13*, 2252.
(7) Liang, Y.; Yap, G. P. A.; Rheingold, A. L.; Theopold, K. H. *Organometallics* **1996**, *15*, 5284.
(8) Lai, S. Y.; Wilson, J. R.; Knight, G. W.; Stevens, J. C.; Chum, P. W. S. US Patent 5,272,236, 1993.
(9) Swogger, K. W. Using Reaction Models to Link Process Conditions to Final Polymer Properties in the INSITE Technology Process. Presented at the Spring A.I.Ch.E. National Meeting, March 14, 1999.
(10) Soares, J. B. P.; Hamielec, A. E. *Macromol. Theory Simul.* **1996**, *5*, 547.
(11) Soares, J. B. P.; Hamielec, A. E. *Macromol. Theory Simul.* **1997**, *6*, 591.
(12) Zhu, S.; Li, D. *Macromol. Theory Simul.* **1997**, *6*, 793.
(13) Pladis, P.; Kiparissides, C. *Chem. Eng. Sci.* **1998**, *53*, 3315.

MA9915935